

AD-A131 949

ELECTRON BEAM TRAJECTORY IN A PHOTOMETER FIELD OF VIEW

1/1

(U) AIR FORCE GEOPHYSICS LAB HANSCOM AFB MA

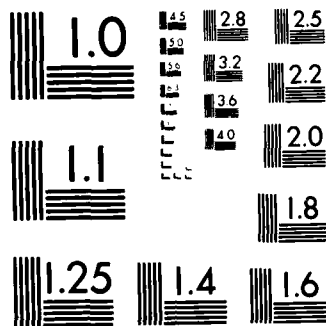
S T LAI ET AL. 16 FEB 83 AFGL-TR-83-0045

UNCLASSIFIED

F/G 12/1

NL





MICROCOPY RESOLUTION TEST CHART
NATIONAL BUREAU OF STANDARDS-1963-A

AD A131949

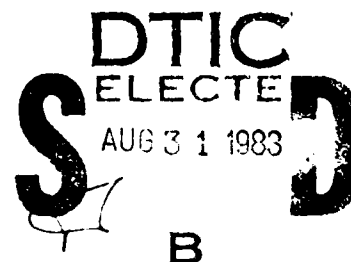
AFGL-TR-83-0045
ENVIRONMENTAL RESEARCH PAPERS, NO. 824



Electron Beam Trajectory in a Photometer Field of View

SHU T. LAI
H. A. COHEN

16 February 1983



Approved for public release; distribution unlimited.

SPACE PHYSICS DIVISION
AIR FORCE GEOPHYSICS LABORATORY
HANSCOM AFB, MASSACHUSETTS 01731

PROJECT 7661

AIR FORCE SYSTEMS COMMAND, USAF

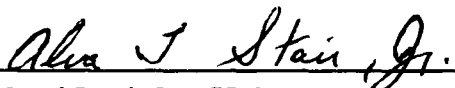


83 08 25 060

DTIC FILE COPY

This report has been reviewed by the ESD Public Affairs Office (PA)
and is releasable to the National Technical Information Service (NTIS).

This technical report has been reviewed and
is approved for publication.


DR. ALVA T. STAIR, Jr
Chief Scientist

Qualified requestors may obtain additional copies from the
Defense Technical Information Center. All others should apply
to the National Technical Information Service.

25511. 25512. 25513. 25514. 25515. 25516. 25517. 25518. 25519. 25520.

REPORT DOCUMENTATION PAGE		READ INSTRUCTIONS BEFORE COMPLETING FORM	
1. REPORT NUMBER	2. GOVT ACCESSION NO.	3. REPORT TYPE AND PERIOD COVERED	4. AUTHOR
5. PERFORMING ORG. REPORT NUMBER	6. AUTHOR (Last, First, Middle)	7. AUTHOR (Last, First, Middle)	8. AUTHOR (Last, First, Middle)
9. PERFORMING ORG. REPORT NUMBER	10. AUTHOR (Last, First, Middle)	11. AUTHOR (Last, First, Middle)	12. AUTHOR (Last, First, Middle)
13. PERFORMING ORG. REPORT NUMBER	14. AUTHOR (Last, First, Middle)	15. AUTHOR (Last, First, Middle)	16. AUTHOR (Last, First, Middle)
17. PERFORMING ORG. REPORT NUMBER	18. AUTHOR (Last, First, Middle)	19. AUTHOR (Last, First, Middle)	20. AUTHOR (Last, First, Middle)
21. PERFORMING ORG. REPORT NUMBER	22. AUTHOR (Last, First, Middle)	23. AUTHOR (Last, First, Middle)	24. AUTHOR (Last, First, Middle)
25. PERFORMING ORG. REPORT NUMBER	26. AUTHOR (Last, First, Middle)	27. AUTHOR (Last, First, Middle)	28. AUTHOR (Last, First, Middle)
29. PERFORMING ORG. REPORT NUMBER	30. AUTHOR (Last, First, Middle)	31. AUTHOR (Last, First, Middle)	32. AUTHOR (Last, First, Middle)
33. PERFORMING ORG. REPORT NUMBER	34. AUTHOR (Last, First, Middle)	35. AUTHOR (Last, First, Middle)	36. AUTHOR (Last, First, Middle)
37. PERFORMING ORG. REPORT NUMBER	38. AUTHOR (Last, First, Middle)	39. AUTHOR (Last, First, Middle)	40. AUTHOR (Last, First, Middle)
41. PERFORMING ORG. REPORT NUMBER	42. AUTHOR (Last, First, Middle)	43. AUTHOR (Last, First, Middle)	44. AUTHOR (Last, First, Middle)
45. PERFORMING ORG. REPORT NUMBER	46. AUTHOR (Last, First, Middle)	47. AUTHOR (Last, First, Middle)	48. AUTHOR (Last, First, Middle)
49. PERFORMING ORG. REPORT NUMBER	50. AUTHOR (Last, First, Middle)	51. AUTHOR (Last, First, Middle)	52. AUTHOR (Last, First, Middle)
53. PERFORMING ORG. REPORT NUMBER	54. AUTHOR (Last, First, Middle)	55. AUTHOR (Last, First, Middle)	56. AUTHOR (Last, First, Middle)
57. PERFORMING ORG. REPORT NUMBER	58. AUTHOR (Last, First, Middle)	59. AUTHOR (Last, First, Middle)	60. AUTHOR (Last, First, Middle)
61. PERFORMING ORG. REPORT NUMBER	62. AUTHOR (Last, First, Middle)	63. AUTHOR (Last, First, Middle)	64. AUTHOR (Last, First, Middle)
65. PERFORMING ORG. REPORT NUMBER	66. AUTHOR (Last, First, Middle)	67. AUTHOR (Last, First, Middle)	68. AUTHOR (Last, First, Middle)
69. PERFORMING ORG. REPORT NUMBER	70. AUTHOR (Last, First, Middle)	71. AUTHOR (Last, First, Middle)	72. AUTHOR (Last, First, Middle)
73. PERFORMING ORG. REPORT NUMBER	74. AUTHOR (Last, First, Middle)	75. AUTHOR (Last, First, Middle)	76. AUTHOR (Last, First, Middle)
77. PERFORMING ORG. REPORT NUMBER	78. AUTHOR (Last, First, Middle)	79. AUTHOR (Last, First, Middle)	80. AUTHOR (Last, First, Middle)
81. PERFORMING ORG. REPORT NUMBER	82. AUTHOR (Last, First, Middle)	83. AUTHOR (Last, First, Middle)	84. AUTHOR (Last, First, Middle)
85. PERFORMING ORG. REPORT NUMBER	86. AUTHOR (Last, First, Middle)	87. AUTHOR (Last, First, Middle)	88. AUTHOR (Last, First, Middle)
89. PERFORMING ORG. REPORT NUMBER	90. AUTHOR (Last, First, Middle)	91. AUTHOR (Last, First, Middle)	92. AUTHOR (Last, First, Middle)
93. PERFORMING ORG. REPORT NUMBER	94. AUTHOR (Last, First, Middle)	95. AUTHOR (Last, First, Middle)	96. AUTHOR (Last, First, Middle)
97. PERFORMING ORG. REPORT NUMBER	98. AUTHOR (Last, First, Middle)	99. AUTHOR (Last, First, Middle)	100. AUTHOR (Last, First, Middle)

Contents

1. INTRODUCTION	5
2. GEOMETRY OF INSTRUMENTATION	6
3. ELECTRON TRAJECTORY—B COORDINATE SYSTEM	8
4. ELECTRON TRAJECTORY—R COORDINATE SYSTEM	9
5. LUMINOSITY	10
6. SCEN ROCKET	13
APPENDIX A: Blockage of Field-of-View by the Horizon	17

Illustrations

1. Geometry of Electron Gun G and Photometer P Mounted on a Section of the Rocket Body	6
2. Geometry of Electron Gun G and Photometer P at Any Instant of Time	7
3. Circular Angular Field-of-View of Photometer	7
4. B Coordinate System	8
5. R Coordinate System	9
6. Typical Behavior of Function $F(t)$	11
7. Electron Beam Trajectory in Photometer Field-of-View	11

Illustrations

8. Circular Electron Trajectory When Initial Beam Velocity is Perpendicular to the Magnetic Field	12
9. Loci of Non-propagation Mode as a Function of Pitch Angle and Azimuth Angle	14
10. Computer Simulation of Electron Beam Trajectory as Viewed at the Photometer on the SCEX Rocket, the Magnetic Field Look-angle in This Simulation is at (0°, 25°)	14
11. Computer Simulation of Electron Beam Trajectory as Viewed at the Photometer on the SCEX Rocket, the Magnetic Field Look-angle in This Simulation is at (0°, 40°)	15
12. Geometrical Factor of Luminosity of the Electron Beam as Viewed by the Photometer on the SCEX Rocket, Beam Energy is 1900 eV	15
13. Geometrical Factor of Luminosity of the Electron Beam as Viewed by the Photometer on the SCEX Rocket, Beam Energy is 8000 eV	16
14. Comparison of the Geometrical Factors for the Cases of 1900-eV and 8000-eV Beam Energies	16
A1. Blockage of Photometer Field-of-View by the Horizon	17
A2. Solution of the Maximum Angle β_{\max}	18

Tables

1. SCEX Photometer Specifications	13
-----------------------------------	----

Accession No.	
NTIS G3417	<input checked="" type="checkbox"/>
DTIC TAB	<input type="checkbox"/>
Unannounced	<input type="checkbox"/>
Justification	
By _____	
Distribution/	
Availability Codes	
Dist	Avail and/or Special
A	



Electron Beam Trajectory in a Photometer Field of View

1. INTRODUCTION

From the inception of the use of electron beams on sounding rocket flights, photometers have been used to measure the light produced by the interaction of the electron beams with the gas surrounding the rocket payload.^{1,2} Since the path of an electron is affected by the earth's magnetic field, the measurable, the luminosity of the beam-gas interaction in the field-of-view of the photometer is also similarly affected. Early experiments tried to minimize these effects by making measurements close to the payload and with a restricted field-of-view for the photometer. For measurements away from the vehicle, and for wide viewing angles, explicit calculations of particle trajectory in the field-of-view of optical devices are necessary for the planning and interpretation of experiments.

Received for publication 14 February 1969

1. J. De Boer, *Philips Research Reports*, 19 (1964) Small Rocket Instrumentation, Delft, The Netherlands; North-Holland Publishing Co., Amsterdam, Holland.

2. J. De Boer, J. H. van der Horst, and J. A. van der Kamp, *Journal of Space Research*, 10 (1963) 101-110; *Journal of Space Research*, 10 (1963) 111-120; *Journal of Space Research*, 10 (1963) 121-130.

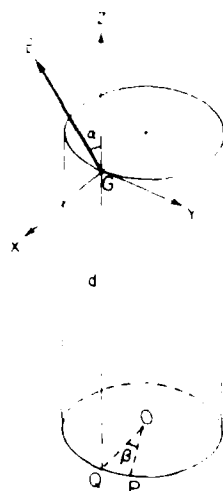
[illegible]

Figure 1. Geometry of Electron Gun G and Photometer P Mounted on a Section of the Rocket Body. The origin of the coordinate system is at G, the z-distance from the gun to the photometer is d .

$$\theta_x = \tan^{-1} \left(\frac{x + \rho - \rho \cos \beta}{z + d} \right), \quad (1)$$

$$\theta_x = \tan^{-1} \left(\frac{x + \rho - \rho \cos \beta}{z + d} \right), \quad (1)$$

$$\nu_y = \tan \left(\frac{y - \rho \sin \beta}{z + d} \right) \quad (2)$$

b'

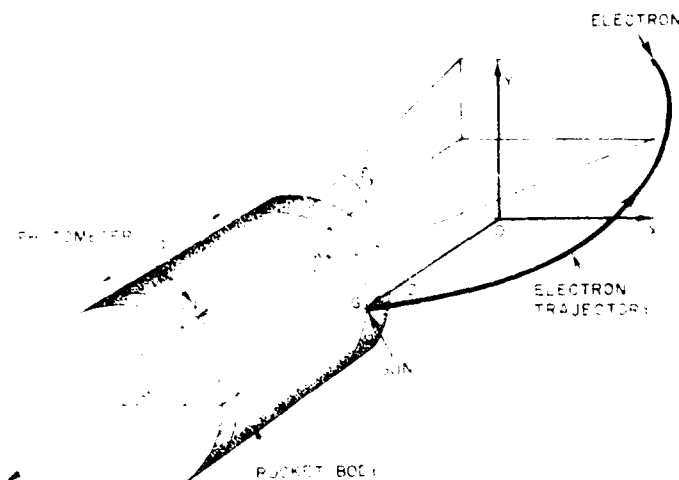


Figure 2. Geometry of Electron Gun G and Photometer P at Any Instant of Time. Beam electron subtends angles θ_x and θ_y at Photometer P.

The field-of-view of the photometer is designed to be limited. It is assumed that the field is circular with the center at $\theta_x(c)$ and $\theta_y(c)$ and radius θ_p . An electron at $\theta_x(t)$, $\theta_y(t)$, would be in the photometer field-of-view if

$$[\theta_x(t) - \theta_x(c)]^2 + [\theta_y(t) - \theta_y(c)]^2 < \theta_p^2. \quad (6)$$

If the above inequality is not satisfied, the electron is outside the photometer field-of-view, as in Figure 3.

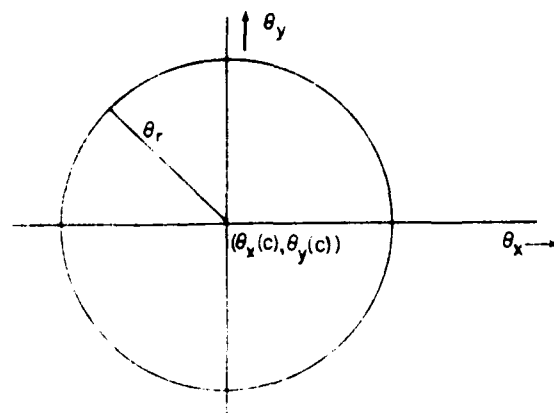


Figure 3. Circular Angular Field-of-View of Photometer.

3. ELECTRON TRAJECTORY-B COORDINATE SYSTEM

The luminosity of the beam atmosphere interaction measured in the photometer's field-of-view is sensitive to the magnetic field orientation with respect to the beam or rocket. Part of the electron trajectory may move in or out of the field-of-view.

In the B system of coordinates as defined in Figure 4, the magnetic field \vec{B} is parallel to the z axis. The vector \vec{V} is the initial beam velocity. The v axis is defined as along $\vec{z} \times \vec{V}$. Thus, \vec{V} lies in the z-x plane. The origin of the beam is at $x=0$, $y=0$, $z=0$. The equation of motion of a beam in the B system is as follows:

$$\begin{bmatrix} x(t) \\ y(t) \\ z(t) \end{bmatrix}_B = \begin{bmatrix} R \sin \omega t \\ R - R \cos \omega t \\ V_{||} t \end{bmatrix} \quad (4)$$

where

$$\omega = \frac{eB}{mc}$$

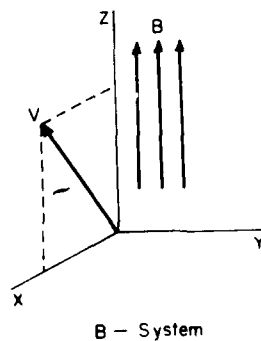


Figure 4. B-Coordinate System. Magnetic field \vec{B} is defined along z-axis

and

$$R = \frac{V_{\perp}}{\omega}$$

where R is gyroradius, ω is gyrofrequency, t is time, and V_{\parallel} and V_{\perp} are the velocity component parallel and perpendicular to the magnetic field respectively. The energy E of the electron is related to the velocity V by $E = 1/2 m V^2$, where m is the mass of electron.

In the B system, the \vec{B} vector is fixed, the \vec{V} vector varies but lies in the z - x plane, and, as the rocket spins, the photometer look-angle varies with time.

4. ELECTRON TRAJECTORY-R COORDINATE SYSTEM

In order to study the electron trajectory in the field-of-view of the photometer, it is more convenient to define an R system of coordinates in which the photometer look-angle is always fixed and the \vec{B} vector varies with time. In the R system (see Figure 5), the z axis is defined as parallel to the rocket axis, y axis is in radial direction, and x completes the right-handed system.

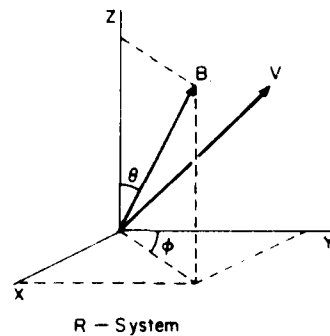


Figure 5. R Coordinate System. The z -axis is parallel to rocket body axis. This is the same coordinate system used in Figure 1.

At time t , let the magnetic field vector \vec{B} be in arbitrary direction, defined by pitch angle $\theta(t)$ and azimuth angle $\phi(t)$ in the R system (see Figure 5).

The equation of motion of a beam electron is obtained in the R system by an orthogonal transformation from Eq. (4) in the B system.

$$\begin{bmatrix} x(t) \\ y(t) \\ z(t) \end{bmatrix}_R = \begin{bmatrix} m_1 & m_2 & m_3 \\ n_1 & n_2 & n_3 \\ p_1 & p_2 & p_3 \end{bmatrix} \begin{bmatrix} x(t) \\ y(t) \\ z(t) \end{bmatrix}_B \quad (5)$$

where m_i , n_i , p_i are the direction cosines of the i -th basis vector of the R system w.r.t. the B system.

In terms of cross products, the transformation equation is as follows:

$$\begin{bmatrix} x(t) \\ y(t) \\ z(t) \end{bmatrix}_R = \begin{bmatrix} (\vec{B} \cdot \vec{V}) \cdot \vec{B} - 1(\vec{B} \cdot \vec{V}) \cdot \vec{B} \\ \vec{B} \cdot \vec{V} \cdot \vec{B} \cdot \vec{V} \\ \vec{B} \cdot \vec{B} \end{bmatrix} \begin{bmatrix} x(t) \\ y(t) \\ z(t) \end{bmatrix}_B \quad (6)$$

In the special case when the magnetic field \vec{B} lies in the plane of the initial electron beam direction and the rocket axis, the transformation equation becomes

$$\begin{bmatrix} x(t) \\ y(t) \\ z(t) \end{bmatrix}_R = \begin{bmatrix} 0 & 1 & 0 \\ -\cos \theta & 0 & \sin \theta \\ \sin \theta & 0 & \cos \theta \end{bmatrix} \begin{bmatrix} x(t) \\ y(t) \\ z(t) \end{bmatrix}_B \quad (7)$$

where

$$\frac{\vec{B}}{B} = (0, \cos \theta, \sin \theta).$$

5. LUMINOSITY

The angular coordinates θ_x and θ_y of an electron as viewed by the photometer are given by Eqs. (1) and (2).

Using the orthogonal transformation equation, Eq. (4), one can write down the angular coordinates (Figure 2), as viewed by a photometer lying at $(0, 0, -d)$:

$$\begin{aligned} \theta_x(t) &= \tan^{-1} \left(\frac{x(t) \cdot \rho - \rho \cos \beta}{z(t) + d} \right) \\ \theta_y(t) &= \tan^{-1} \left(\frac{y(t) - \rho \sin \beta}{z(t) + d} \right) \end{aligned} \quad (8)$$

The electron would lie in the photometer field-of-view if Eq. (3) is satisfied (see Figure 3). Equivalently, let us define a function $F(t)$:

$$F(t) = \frac{1}{r^2} = \frac{1}{r^2} \left\{ [x_X(t) - x_X(c)]^2 + [y_V(t) - y_V(c)]^2 \right\}.$$

If Eq. (3) is satisfied, then the function $F(t)$ is positive, (see Figures 6 and 7).

$$F(t) > 0. \quad (9)$$

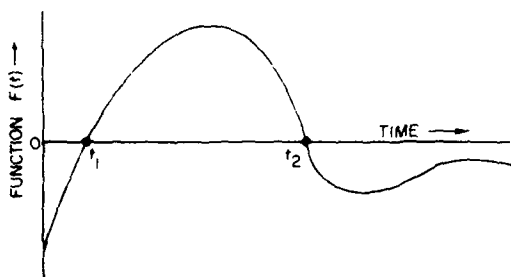


Figure 6. Typical Behavior of Function $F(t)$. The beam electron is in the photometer field-of-view during the period t_1 to t_2 .

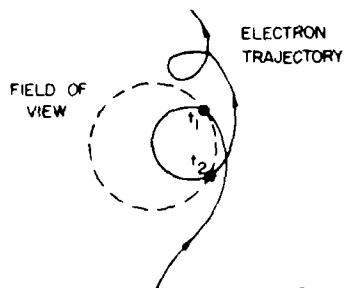


Figure 7. Electron Beam Trajectory in Photometer Field-of-View. The beam entering field-of-view (dashed circle) at t_1 and leaves at t_2 .

If the electron interacts with a gas atom, or molecule, to create ionization or excitation, the luminosity $L(E)$ measured at the photometer is proportional to the inverse square of the distance $s(t)$ of the electron from the photometer.

$$L(t) = N \int_{t_1}^{t_2} L(E) \frac{1}{s^2(t)} dt \quad (10)$$

$$L(t) = N \int_{t_1}^{t_2} L(E) \frac{1}{s^2(t)} dt$$

where N is a proportionality constant, V is the velocity of the electron, and $\sigma(E)$ is the cross-section of ionization and excitation. It is assumed that no significant energy loss ($\Delta E/E \ll 1$) takes place along the beam while in the photometer field-of-view. $\mathbb{H}(x)$ is a step function:

$$\mathbb{H}(x) = \begin{cases} 1 & \text{if } x > 0 \\ 0 & \text{if } x \leq 0 \end{cases}.$$

From Eq. (10), one obtains the geometric factor G as follows:

$$L(E) = N V(E) \sigma(E) G$$

where

$$G = \sum_{i=1}^{\infty} \int_{t_{2i-1}}^{t_{2i}} dt \frac{1}{s^2(t)}$$

$$s(t) = [x^2(t) + v^2(t) + (z + d)^2]^{1/2}.$$

When the initial velocity vector \vec{V} of the electron is perpendicular to the magnetic field vector \vec{B} , the beam forms a circular path. The condition is

$$\vec{B} \cdot \vec{V} = 0. \quad (11)$$

Every electron injected into the path would stay in the path and never propagate away (see Figure 8). This is a nonpropagation mode. The luminosity $L(E)$ for this mode is high, because $s^{-2}(t)$ does not decrease with time.

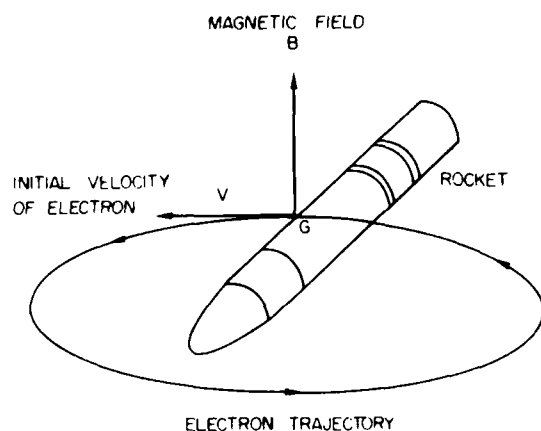


Figure 8. Circular Electron Trajectory When Initial Electron Velocity is Perpendicular to the Magnetic Field

The above condition agrees with the experimental result of Israelson and Winckler³ who detected a substantial increase in photon flux at 90° pitch angle in the Echo 2 rocket beam experiment.

6. SCEx ROCKET

As an example, for the SCEx rocket^{*} experiment the specifications of the photometer on-board is given in Table 1.

Table 1. SCEx Photometer Specifications

Photometer rotation angle β	= 0°
Photometer distance from gun (d)	= 119 cm
Center of field-of-view [$\theta_x(c)$, $\theta_y(c)$]	= [0°, 20°]
Radius of field-of-view θ_r	= 15°

The condition of Eq. (11) for nonpropagation modes to exist becomes

$$\sin \theta \cos \phi + \cos \theta = 0 \quad (12)$$

where θ and ϕ are rocket pitch and azimuth angles. The solutions of Eq. (12) are plotted in Figure 9.

In Figure 9, the pitch angle actually runs only from 0° to 180° because it is a cone angle. The azimuth angle ϕ at 180° is the same as -180° because it is a rotation angle. Solutions exist only for a range of values of pitch angle.

Examples of electron beam trajectories as viewed at the SCEx photometer are presented in Figures 10 and 11. Three-dimensional plots of luminosity, for the case of SCEx, as a function of θ and ϕ , are shown in Figures 12 and 13. The location of the spikes should fall on a continuous curve given in Eq. (12) (Figure 9) but computer calculation requires the use of grid points which are discrete. Therefore the singularities do not look like a continuous wall, but appear as spikes. The 1900-eV case gives a generally higher (about 2 to 3 times) luminosity than the

3. Israelson, G., and Winckler, J.R. (1975) Measurement of 3914-Å light production and electron scattering from electron beams artificially injected into the ionosphere, J. Geophys. Res. 80:No. 25:3709-3712.

* NASA Rocket 27,045, launched on 27 January 1982, from Churchill, Canada.

4000-ew, and give the following equations that show that the electron beam is in focus:

Electron beam diameter at 1000 ft = $1000 \times \frac{1}{1000} = 1$ ft. (1000 ft. is the distance from the SCEN Rocket to the photometer, and 1000 is the magnification factor.)

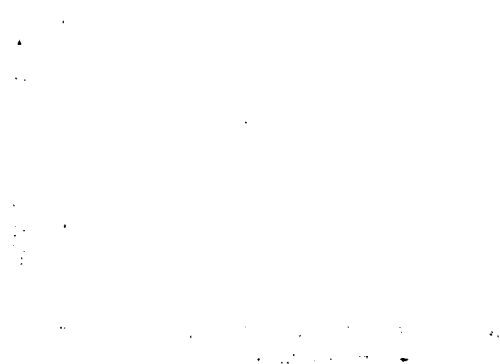


Figure 9. Plot of
Nominatation Mode
as a function of Pitch
Angle and Azimuth Angle

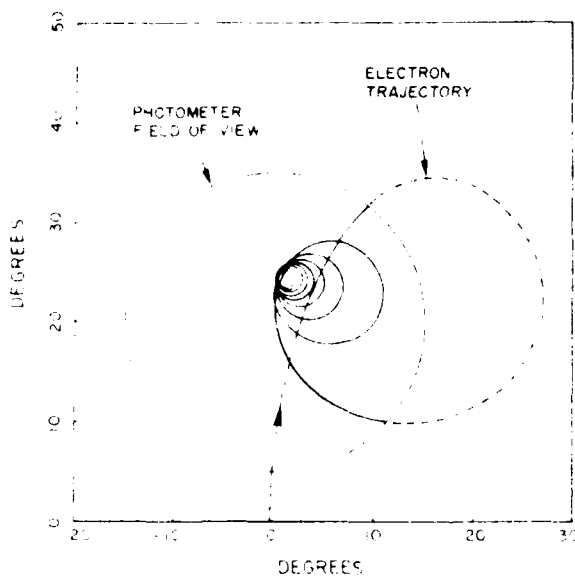


Figure 10. Computer
Simulation of Electron Beam
Trajectory as Viewed at the
Photometer on the SCEN
Rocket, the Magnetic Field
Look-angle in This Simulation
is 0°, 25°. The dashed
part of the trajectory is
outside the circular field of
view.

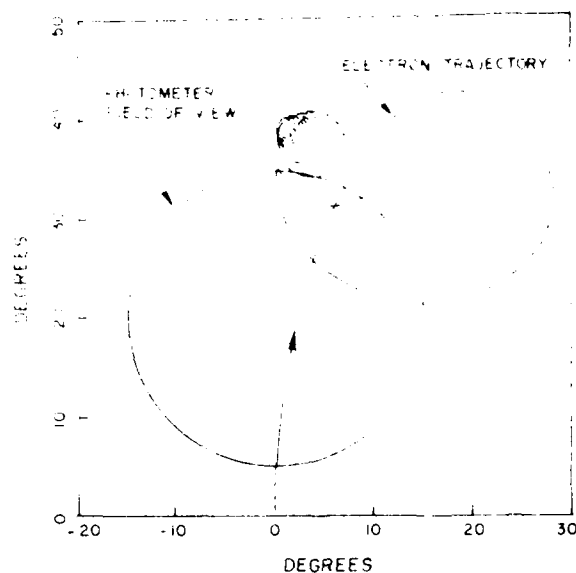


Figure 11. Electron Trajectory as Viewed by the Photometer on the SC EX Rocket. The Pitch Angle is 45°. The Photometer is at 10°. However, the Maximum Pitch Angle is 15°. Simulation is at 40°. The dashed part of the trajectory is outside the photometer field of view.

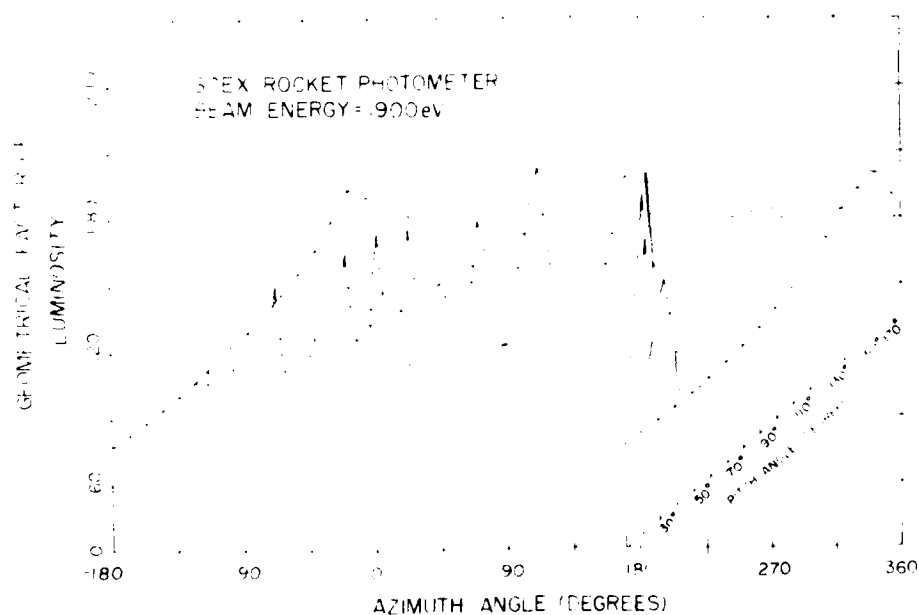


Figure 12. Geometrical Factor of Luminosity of the Electron Beam as Viewed by the Photometer on the SC EX Rocket, Beam Energy is 1900 eV. The functional dependence on pitch and azimuth angles are plotted

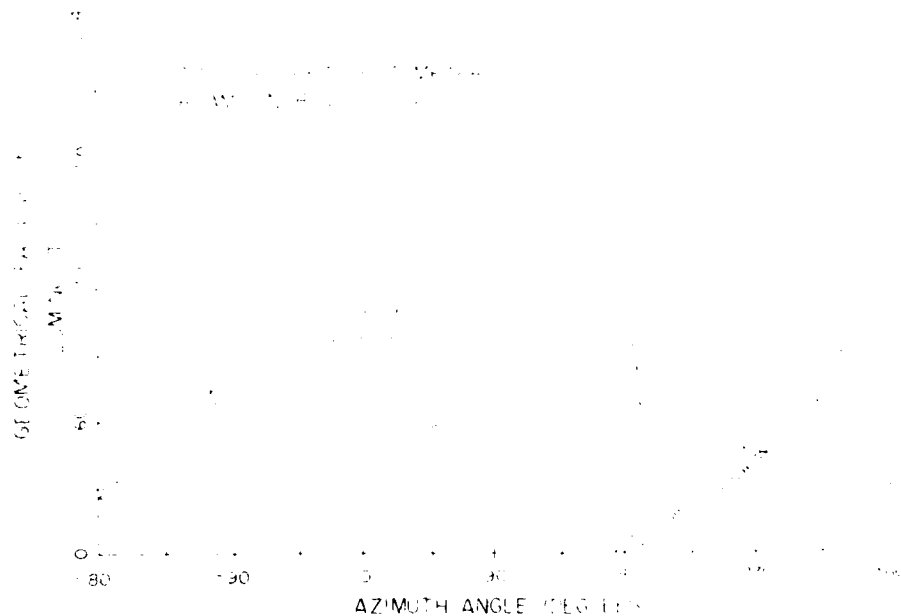


Figure 13. Geometrical Factor of Luminosity of the Electron Beam as Viewed by the Photometer on the SCEN Rocket, Beam Energy is 8000 eV. The functional dependence on pitch and azimuth angles are plotted.

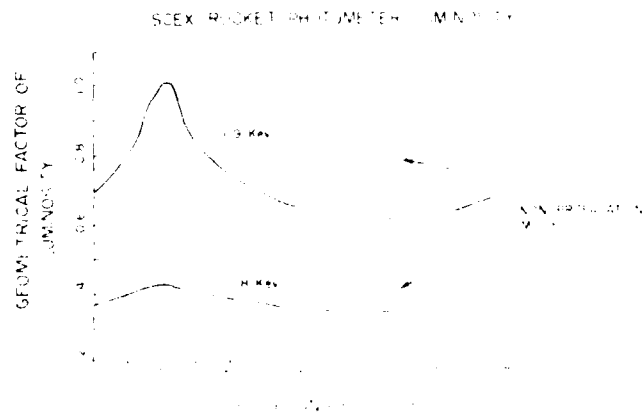


Figure 14. Comparison of the Geometrical Factor of Luminosity of the Electron Beam as Viewed by the SCEN Rocket, Beam Energy is 1000 eV and 8000 eV. Beam Energy is 1000 eV and 8000 eV. The functional dependence on pitch and azimuth angles are plotted.

Appendix A

Blockage of Field-of-View by the Horizon

The blockage of the field-of-view, for a wide angle photometer P, is determined by the horizon. For the geometry shown in Figure A1, the equation of the horizon is

$$y = mx + c,$$

where

$$m = -\tan \beta$$

$$c = \rho(\sec \beta - 1).$$

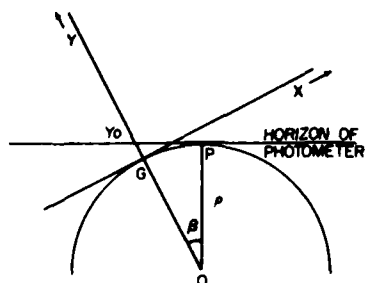


Figure A1. Blockage of Photometer Field-of-View by the Horizon

If at $x = 0$, blockage is desired to be below y_0 , then

$$\rho(\sec \beta - 1) < y_0,$$

that is

$$\frac{1}{\cos \beta} < \frac{y_0 + \rho}{\rho}.$$

This determines the maximum β , (see Figure A2).

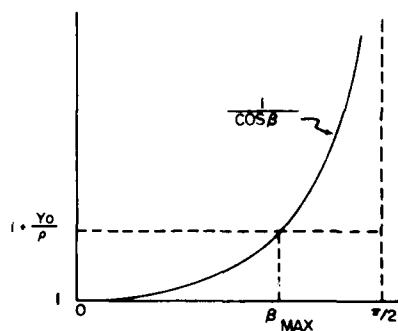


Figure A2. Solution of the Maximum Angle β_{\max}

END

FILMED

9-83

DTIC